CHAPTER 2

THEORETICAL MODELING OF BACKSCATTER USING FOCUSED SOURCES

Most of the previous models used to analyze the backscattered waveforms have assumed plane waves incident on the scattering region (i.e., inside focal zone of weakly focused source) while only considering diffraction effects in the transverse plane [*Lizzi et al.*, 1983; *Insana et al.*, 1990; *Lizzi et al.*, 1997a]. Diffraction effects along the beam axis have been neglected. Other authors included a complete Green's function description of the source when determining the scattered field [*Madsen et al.*, 1984; *Insana et al.*, 1986; *Wear et al.*, 1989; *Chen et al.*, 1993]. In their calculations, they assumed that the excitation across the entire surface of the source was known or could be accurately determined. They also assumed that the scatterers were a sufficient distance from the source, and the field was approximately constant across the scatterer. Unfortunately, the resulting equations were cumbersome and required precise knowledge of the source's excitation in order to solve for the required fields. As a result, it is difficult to use their results when experimentally calibrating a focused source for the purpose of estimating scatterer size. Furthermore, their analysis still does not provide analytical insight into the effects of beam diffraction. Recently, *Gerig et al.* [2003] proposed using a reference phantom containing spherical glass bead scatterers to obtain a reference spectrum that could potentially account for focusing. However, the ability of the reference phantom technique to correct for focusing has not been fully evaluated, and the reference phantom technique still does not provide any analytical insight.

Due to these limitations, most investigators use large f-number transducers in their backscatter analyses where diffraction effects along the beam axis can be neglected over the size of the region of interest (i.e., time gated region). Reducing the length of the time gate to allow for smaller f-number transducers while still ignoring diffraction effects is not feasible because both the accuracy and precision of the scatterer size (effective radius of spherically symmetric

scatterer) estimates degrade when the window length is too small. This is potentially restrictive in diagnostic imaging systems where smaller f-numbers may be desirable to improve the spatial resolution of the quantitative ultrasound image. Hence, the purpose of this chapter is to allow for the use of focused sources when quantifying the backscattered ultrasound waveforms before addressing the problem of unknown attenuation along the propagation path.

In this chapter, the expected backscattered voltage from a region of randomly positioned uniform scatterers is rederived without the plane wave approximation. Instead, it is assumed that the velocity potential field near the focus can be accurately modeled as a three-dimensional Gaussian beam while continuing to assume that the scatterers are at a sufficient distance from the source, and the field is approximately constant across the scatterer. The analysis is also extended to find the expected backscattered intensity through a planarly layered low-contrast attenuating medium. After completing the theoretical derivations, the traditional approach for estimating the scatterer size based on the model will be discussed. Throughout the analysis, the effects of shear wave propagation are neglected in order to simplify the mathematical expressions.

2.1 Derivation of Backscattered Voltage from Tissue Microstructure

The scattering model begins by assuming that the tissue is a random distribution of particles. From a Green's functions analysis, it can be shown that the scattered field from the particles should be given by [*Morse and Ingard*, 1968]

$$p_s(\vec{r}) = \iiint_{V'} \left\{ \tilde{k}_1^2 \gamma_\kappa(\vec{r}\,') p_{tot}(\vec{r}\,') g(\vec{r},\vec{r}\,') + \gamma_\rho(\vec{r}\,') \nabla' p_{tot}(\vec{r}\,') \cdot \nabla' g(\vec{r},\vec{r}\,') \right\} d\vec{r}\,', \qquad (2.1)$$

where V' is some volume containing the scatterers contributing to the scattered signal, $g(\vec{r},\vec{r}\,')$ is the Green's function for the background medium, p_{tot} is the total pressure field, and $\tilde{k}_1$ is the complex wavenumber of the background about the scatterer. The functions γ_κ and γ_ρ reflect spatial perturbations in the compressibility κ and density ρ due to the scatterers and are given by [*Morse and Ingard*, 1968]

$$\begin{aligned} \gamma_\kappa(\vec{r}) &= \frac{\kappa_s(\vec{r}) - \kappa}{\kappa} \\ \gamma_\rho(\vec{r}) &= \frac{\rho_s(\vec{r}) - \rho}{\rho_s(\vec{r})}. \end{aligned} \qquad (2.2)$$

In this equation, κ_s and ρ_s are the compressibility and density of the scatterers while κ and ρ are the compressibility and density of the background medium. The effect of some variations in κ and ρ in the background region can be captured by the Green's function, so the only requirement is that κ and ρ be approximately constant for some small volume about the scatterers.

At this point in the derivation, it is generally assumed that the medium away from the scatterers is homogeneous resulting in the use of the homogeneous Green's function [*Gore and Leeman*, 1977; *Lizzi et al*., 1983; *Nassiri and Hill*, 1986; *Insana et al.*, 1990]. This assumption is not valid for biological tissue where the scattering region of interest is often buried beneath many other tissue types. However, if we assume that multiple scattering between the layers can be neglected, then the homogeneous Green's function can be used with slight modification to account for the sound transmission into the different layers. As an example, consider the Green's function for a point source imbedded in a planarly layered medium consisting of three layers as shown in Figure 2.1.

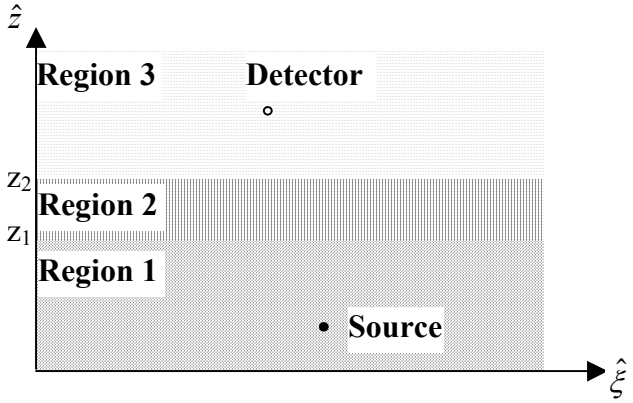

Figure 2.1: Planarly layered medium for Green's function calculation where the boundaries between the layers are defined as planes along the z-axis ($\hat{z}$) that are infinite in extent in the ξ-plane ($\hat{\xi}$).

The "field" in Region 1 generated by the point source at location $\vec{r}_s$ is given by [*Morse and Ingard*, 1968]

$$g_1(\vec{r},\vec{r}_s) = \frac{1}{4\pi|\vec{r}-\vec{r}_s|}\exp\left[\left(ik_1-\alpha_1\right)|\vec{r}-\vec{r}_s|\right], \tag{2.3}$$

where k_1 and α_1 are the wavenumber and attenuation in Region 1. This field can then be propagated through the other regions by decomposing it into a set of plane waves according to [*Chew*, 1995]

$$\begin{aligned}\frac{\exp\left(\left(ik_1-\alpha_1\right)\left|\vec{r}-\vec{r}_s\right|\right)}{\left|\vec{r}-\vec{r}_s\right|} &= \frac{\exp\left(i\tilde{k}_1\left|\vec{r}-\vec{r}_s\right|\right)}{\left|\vec{r}-\vec{r}_s\right|} \\ &= \frac{i}{2}\int_{-\infty}^{\infty} dk_\xi \frac{k_\xi H_0^{(1)}\left(k_\xi\left|\xi-\xi_s\right|\right)\exp\left(i\tilde{k}_{1z}\left|z-z_s\right|\right)}{\tilde{k}_{1z}}\end{aligned}. \tag{2.4}$$

In this equation, $\tilde{k}_1$ is the complex wavenumber in Region 1 with k_ξ and $\tilde{k}_{1z}$ related to $\tilde{k}_1$ by the relation [*Chew*, 1995]

$$\tilde{k}_{1z} = \left(\tilde{k}_1^2 - k_\xi^2\right)^{\frac{1}{2}}. \tag{2.5}$$

Due to the planar geometry, the k_ξ values for each term in the integrand remain unchanged as the waves propagate through the planar geometry. Because multiple reflections are neglected, transmission through the layers can be accomplished by simply including the appropriate transmission coefficient between the layers for each of the plane waves. Hence, the field at the detector is simply given by

$$g\left(\vec{r}_d,\vec{r}_s\right) = \frac{i}{8\pi}\int_{-\infty}^{\infty} dk_\xi T_{12}T_{23}\frac{k_\xi H_0^{(1)}\left(k_\xi\left|\xi_d-\xi_s\right|\right)}{\tilde{k}_{1z}} e^{i\tilde{k}_{1z}\left|z_1-z_s\right|+i\tilde{k}_{2z}\left|z_2-z_1\right|+i\tilde{k}_{3z}\left|z_d-z_2\right|}, \tag{2.6}$$

where

$$\begin{aligned}T_{12} &= \frac{2\rho_2 c_2\tilde{k}_2\tilde{k}_{1z}}{\rho_2 c_2\tilde{k}_2\tilde{k}_{1z}+\rho_1 c_1\tilde{k}_1\tilde{k}_{2z}} \\ T_{23} &= \frac{2\rho_3 c_3\tilde{k}_3\tilde{k}_{2z}}{\rho_3 c_3\tilde{k}_3\tilde{k}_{2z}+\rho_2 c_2\tilde{k}_2\tilde{k}_{3z}}\end{aligned}. \tag{2.7}$$

If the model were to be extended to *N*-layers, the only modification would be the inclusion of the additional transmission coefficients from each region and the multiplication of the required phase terms, $e^{i\tilde{k}_{jz}\left|z_j-z_i\right|}$, accounting for propagation within each region.

Even though Equation (2.6) provides the desired Green's function, it would be more useful if the integration could be solved explicitly. Therefore, we will assume that the sound speed and attenuation of the different regions are comparable allowing the complex wavenumbers in the $\hat{z}$-direction to be written as

$$\begin{aligned}
\widetilde{k}_{1z} = \widetilde{k}_z + d\widetilde{k}_{1z} \Rightarrow \widetilde{k}_{1z}^2 &\cong \widetilde{k}_z^2 + 2\widetilde{k}_z d\widetilde{k}_{1z} = \widetilde{k}^2 - k_\xi^2 + 2\widetilde{k}_z d\widetilde{k}_{1z} \\
\Rightarrow \widetilde{k}_1^2 &= \widetilde{k}^2 + 2\widetilde{k}_z d\widetilde{k}_{1z} \cong \widetilde{k}^2 + 2\widetilde{k} d\widetilde{k}_1 \\
\Rightarrow d\widetilde{k}_{1z} = \frac{\widetilde{k} d\widetilde{k}_1}{\widetilde{k}_z} &\Rightarrow \widetilde{k}_{1z} \cong \widetilde{k}_z + \frac{\widetilde{k} d\widetilde{k}_1}{\widetilde{k}_z} \\
\widetilde{k}_{2z} &\cong \widetilde{k}_z + \frac{\widetilde{k} d\widetilde{k}_2}{\widetilde{k}_z} \\
\widetilde{k}_{3z} &\cong \widetilde{k}_z + \frac{\widetilde{k} d\widetilde{k}_3}{\widetilde{k}_z},
\end{aligned} \tag{2.8}$$

where the $d\widetilde{k}_i$ are the differences from the approximate homogeneous value $\widetilde{k}$ in the complex wavenumber for each layer (i.e., $d\widetilde{k}_i = \widetilde{k} - \widetilde{k}_i$). Furthermore, keeping only the 0^{th}-order perturbations in the transmission coefficients since they are amplitude terms yields

$$\begin{aligned}
T_{12} &\cong \frac{2\rho_2 c_2}{\rho_2 c_2 + \rho_1 c_1} \\
T_{23} &\cong \frac{2\rho_3 c_3}{\rho_3 c_3 + \rho_2 c_2}
\end{aligned}. \tag{2.9}$$

Substituting these values into the Green's function then yields

$$g(\vec{r}_d, \vec{r}_s) \cong \frac{i}{8\pi} T_{12} T_{23} \int_{-\infty}^{\infty} dk_\xi \frac{k_\xi H_0^{(1)}\left(k_\xi \left|\xi_d - \xi_s\right|\right)}{\widetilde{k}_z} e^{i\widetilde{k}\frac{d\widetilde{k}_1}{\widetilde{k}_z}\left|z_1 - z_s\right| + i\widetilde{k}\frac{d\widetilde{k}_2}{\widetilde{k}_z}\left|z_2 - z_1\right| + i\widetilde{k}\frac{d\widetilde{k}_3}{\widetilde{k}_z}\left|z_d - z_2\right|} e^{i\widetilde{k}_z\left|z_d - z_s\right|}. \tag{2.10}$$

The integral in Equation (2.10) can now be solved using the method of stationary phase with [*Chew*, 1995]

$$\begin{aligned}
g(\vec{r}_d, \vec{r}_s) &= \int_{-\infty}^{\infty} G_{sp}\left(\Lambda, k_\xi\right) F_{sp}\left(k_\xi\right) dk_\xi \\
G_{sp}\left(\Lambda, k_\xi\right) &= \frac{i}{8\pi} T_{12} T_{23} \frac{k_\xi H_0^{(1)}\left(k_\xi \left|\xi_d - \xi_s\right|\right)}{\widetilde{k}_z} e^{i\left|z_d - z_s\right|\widetilde{k}_z} \\
F_{sp}\left(k_\xi\right) &= e^{i\left(\widetilde{k}\frac{d\widetilde{k}_1}{\widetilde{k}_z}\left|z_1 - z_s\right| + \widetilde{k}\frac{d\widetilde{k}_2}{\widetilde{k}_z}\left|z_2 - z_1\right| + \widetilde{k}\frac{d\widetilde{k}_3}{\widetilde{k}_z}\left|z_d - z_2\right|\right)}
\end{aligned}. \tag{2.11}$$

Under these conditions, the stationary phase point can be found at [*Chew*, 1995]

$$k_{\xi s} = \frac{\widetilde{k}\left|\xi_d - \xi_s\right|}{\sqrt{\left|\xi_d - \xi_s\right|^2 + \left|z_d - z_s\right|^2}}. \tag{2.12}$$

Hence, the integral for the Green's function can be approximated to first order by

$$
\begin{aligned}
g(\vec{r}_d,\vec{r}_s) &\approx F_{sp}\left(k_{\xi s}\right)\int_{-\infty}^{\infty} G_{sp}\left(\Lambda,k_\xi\right)dk_\xi \\
&= \frac{i}{8\pi}T_{12}T_{23}e^{i\left(\tilde{k}\frac{d\tilde{k}_1}{\tilde{k}_{zs}}|z_1-z_s|+\tilde{k}\frac{d\tilde{k}_2}{\tilde{k}_{zs}}|z_2-z_1|+\tilde{k}\frac{d\tilde{k}_3}{\tilde{k}_{zs}}|z_d-z_2|\right)}\int_{-\infty}^{\infty}\frac{k_\xi H_0^{(1)}\left(k_\xi|\xi_d-\xi_s|\right)}{\tilde{k}_z}e^{i|z_d-z_s|\tilde{k}_z}dk_\xi \\
&= \frac{1}{4\pi}\frac{e^{i\tilde{k}|\vec{r}_d-\vec{r}_s|}}{|\vec{r}_d-\vec{r}_s|}T_{12}T_{23}e^{i\left(\tilde{k}\frac{d\tilde{k}_1}{\tilde{k}_{zs}}|z_1-z_s|+\tilde{k}\frac{d\tilde{k}_2}{\tilde{k}_{zs}}|z_2-z_1|+\tilde{k}\frac{d\tilde{k}_3}{\tilde{k}_{zs}}|z_d-z_2|\right)},
\end{aligned}
\tag{2.13}
$$

where

$$
\tilde{k}_{zs}=\sqrt{\tilde{k}^2-k_{\xi s}^2}\,. \tag{2.14}
$$

Equation (2.13) can be further simplified by assuming that $k_{\xi s}$ is small compared to $\tilde{k}$ as would be the case for scattering regions located directly underneath the detector deep within the tissue. With this assumption,

$$
\frac{d\tilde{k}_i}{\tilde{k}_{zs}}=\frac{d\tilde{k}_i}{\tilde{k}\sqrt{1-\frac{k_{\xi s}^2}{\tilde{k}^2}}}\cong\frac{d\tilde{k}_i}{\tilde{k}}\left(1+\frac{k_{\xi s}^2}{2\tilde{k}^2}\right)\cong\frac{d\tilde{k}_i}{\tilde{k}}, \tag{2.15}
$$

yielding a Green's function of

$$
g(\vec{r}_d,\vec{r}_s)\cong\frac{1}{4\pi}\frac{e^{i\tilde{k}|\vec{r}_d-\vec{r}_s|}}{|\vec{r}_d-\vec{r}_s|}T_{12}T_{23}e^{i\left(d\tilde{k}_1|z_1-z_s|+d\tilde{k}_2|z_2-z_1|+d\tilde{k}_3|z_d-z_2|\right)}. \tag{2.16}
$$

Therefore, the layered medium tends to modify the amplitude of the signal by the transmission coefficients between the layers, and to modify the phase by a perturbation associated with the distance spent within each layer. Based on this result, the optimal value of $\tilde{k}$ is a weighted average related to the distance covered by the wave within each layer.

Now that the appropriate Green's function for the layered medium has been found, Equation (2.1) can be solved to find the expected scattered field in Region 3. At this point, it will be assumed that the scatterers of interest are weak scatterers that satisfy the Born approximation. As a result, p_{tot} can be replaced by only the incident field on the scatterers given by [*Morse and Ingard*, 1968]

$$
p_{inc}(\vec{r}\,')=-2i\omega\rho_3\iint_{S_T}u_z(\vec{r}_T)g_T(\vec{r}\,',\vec{r}_T)d\vec{r}_T\,, \tag{2.17}
$$

where u_z is the normal particle velocity at location $\vec{r}_T$ on the aperture plane, S_T, of the excitation transducer. $g_T(\vec{r}',\vec{r}_T)$ can be found by analysis similar to that used to find the Green's function in Equation (2.16) and is given by

$$g_T(\vec{r}',\vec{r}_T) \cong \frac{1}{4\pi}\frac{e^{i\tilde{k}|\vec{r}_T-\vec{r}'|}}{|\vec{r}_T-\vec{r}'|} T_{21}T_{32} e^{i\left(d\tilde{k}_1|z_1-z'|+d\tilde{k}_2|z_2-z_1|+d\tilde{k}_3|z_T-z_2|\right)}. \tag{2.18}$$

Therefore, the scattered field at detector location $\vec{r}_d$ is given by

$$p_s(\vec{r}_d) = -2i\omega\rho_3 \iint_{S_T} d\vec{r}_T \iiint_{V'} \begin{Bmatrix} \tilde{k}_1^2 \gamma_\kappa(\vec{r}') u_z(\vec{r}_T) g_T(\vec{r}',\vec{r}_T) g(\vec{r}_d,\vec{r}') \\ +\gamma_\rho(\vec{r}') u_z(\vec{r}_T) \nabla' g_T(\vec{r}',\vec{r}_T)\cdot\nabla' g(\vec{r}_d,\vec{r}') \end{Bmatrix} d\vec{r}'. \tag{2.19}$$

Equation (2.19) can be further simplified by

$$\begin{aligned} \nabla' g(\vec{r},\vec{r}') &\cong \frac{1}{4\pi} T_{12}T_{23} e^{i\left(d\tilde{k}_2|z_2-z_1|+d\tilde{k}_3|z-z_2|\right)} \nabla'\left(\frac{e^{i\tilde{k}|\vec{r}-\vec{r}'|+id\tilde{k}_1|z_1-z'|}}{|\vec{r}-\vec{r}'|}\right) \\ &= \frac{1}{4\pi} T_{12}T_{23} \frac{e^{i\tilde{k}|\vec{r}-\vec{r}'|}}{|\vec{r}-\vec{r}'|} e^{i\left(d\tilde{k}_1|z_1-z'|+d\tilde{k}_2|z_2-z_1|+d\tilde{k}_3|z-z_2|\right)} \left[\left(i\tilde{k}\nabla'|\vec{r}-\vec{r}'| \mp \hat{z}\left(id\tilde{k}_1\right), \begin{matrix} z_1>z' \\ z_1<z' \end{matrix}\right) - \frac{\nabla'|\vec{r}-\vec{r}'|}{|\vec{r}-\vec{r}'|}\right] \\ &\cong g(\vec{r},\vec{r}')\left[i\tilde{k}\nabla'|\vec{r}-\vec{r}'| \mp \hat{z}\left(id\tilde{k}_1\right), \begin{matrix} z_1>z' \\ z_1<z' \end{matrix}\right]. \end{aligned} \tag{2.20}$$

Hence, $\nabla' g_T(\vec{r}',\vec{r}_T)\cdot\nabla' g(\vec{r}_d,\vec{r}')$ becomes

$$\begin{aligned} \nabla' g_T(\vec{r}',\vec{r}_T)\cdot\nabla' g(\vec{r}_d,\vec{r}') &\cong \begin{cases} g_T(\vec{r}',\vec{r}_T)\left[i\tilde{k}\nabla'|\vec{r}_T-\vec{r}'| \mp \hat{z}\left(id\tilde{k}_1\right)\right]\cdot \\ g(\vec{r}_d,\vec{r}')\left[i\tilde{k}\nabla'|\vec{r}_d-\vec{r}'| \mp \hat{z}\left(id\tilde{k}_1\right)\right] \end{cases} \begin{matrix} z_1>z' \\ z_1<z' \end{matrix} \\ &\cong \left\{-\tilde{k}^2 g_T(\vec{r}',\vec{r}_T) g(\vec{r}_d,\vec{r}')\left(\nabla'|\vec{r}_T-\vec{r}'|\right)\cdot\left(\nabla'|\vec{r}_d-\vec{r}'|\right)\right\}, \end{aligned} \tag{2.21}$$

where once again, use has been made of the assumption that the perturbations in $\tilde{k}$ between the layers are small.

In order to make the above equations more tractable, the origin is placed within the scattering region, and it is assumed that the dimensions of our scattering region are small relative to its distance from the transducer and the detector. The validity of this approximation increases with decreasing window length used to gate the signal in the time domain, increasing focusing (i.e., decreasing f-numbers), and increasing focal length. In this case, the calculations are simplified by [*Morse and Ingard*, 1968]

$$\begin{aligned}
\left|\vec{r}_T-\vec{r}'\right| &= \sqrt{r_T^2-2\left(x_Tx'+y_Ty'+z_Tz'\right)+r'^2} = \sqrt{r_T^2-2\left(\vec{r}_T\cdot\vec{r}'\right)+r'^2} \\
&\cong r_T\left(1-\frac{1}{r_T^2}\left(\vec{r}_T\cdot\vec{r}'\right)+\frac{r'^2}{2r_T^2}-\frac{1}{2r_T^4}\left(\vec{r}_T\cdot\vec{r}'\right)^2\right)\cong r_T-\frac{\vec{r}_T}{r_T}\cdot\vec{r}' \qquad (2.22)\\
\left|\vec{r}_d-\vec{r}'\right| &\cong r_d-\frac{\vec{r}_d}{r_d}\cdot\vec{r}'.
\end{aligned}$$

Also, assuming that the transducer and detector are in approximately the same direction (i.e., different elements of the same source), then

$$\left(\frac{\vec{r}_d\cdot\vec{r}_T}{r_dr_T}\right)\approx 1. \qquad (2.23)$$

Hence, Equation (2.21) becomes

$$\nabla' g_T\left(\vec{r}',\vec{r}_T\right)\cdot\nabla' g\left(\vec{r}_d,\vec{r}'\right)\cong\left\{-\tilde{k}^2 g_T\left(\vec{r}',\vec{r}_T\right)g\left(\vec{r}_d,\vec{r}'\right)\right\}, \qquad (2.24)$$

yielding scattered field at the detector of

$$\begin{aligned}
p_s\left(\vec{r}_d\right) &= -2i\omega\rho_3\iint_{S_T}d\vec{r}_T u_z\left(\vec{r}_T\right)\iiint_{V'}g_T\left(\vec{r}',\vec{r}_T\right)g\left(\vec{r}_d,\vec{r}'\right)\left\{\tilde{k}_1^2\gamma_\kappa\left(\vec{r}'\right)-\tilde{k}^2\gamma_\rho\left(\vec{r}'\right)\right\}d\vec{r}' \\
&\cong\left(-2i\omega\rho_3\right)\left(\frac{\tilde{k}}{4\pi}\right)^2\frac{T_{12}T_{21}T_{32}T_{23}e^{i\tilde{k}r_d}e^{2id\tilde{k}_2|z_2-z_1|+id\tilde{k}_3|z_d-z_2|}}{r_d}\cdot \qquad (2.25)\\
&\iint_{S_T}d\vec{r}_T\left(\frac{u_z\left(\vec{r}_T\right)e^{i\tilde{k}r_T}e^{id\tilde{k}_3|z_T-z_2|}}{r_T}\iiint_{V'}d\vec{r}'\left\{\gamma_\kappa\left(\vec{r}'\right)-\gamma_\rho\left(\vec{r}'\right)\right\}e^{\left(2id\tilde{k}_1|z_1-z'|\right)-i\tilde{k}\vec{r}'\cdot\left(\frac{\vec{r}_d}{r_d}+\frac{\vec{r}_T}{r_T}\right)}\right).
\end{aligned}$$

Equation (2.25) can also be generalized to an *N*-layered medium yielding

$$\begin{aligned}
p_s\left(\vec{r}_d\right) &= \left(-2i\omega\rho_N\right)\left(\frac{\tilde{k}}{4\pi}\right)^2\prod_{j=2}^{N-1}\left(T_{j,j-1}T_{j-1,j}e^{2id\tilde{k}_j\left|z_j-z_{j-1}\right|}\right)T_{N,N-1}T_{N-1,N}e^{id\tilde{k}_N|z_d-z_{N-1}|}\frac{e^{i\tilde{k}r_d}}{r_d}\cdot \\
&\iint_{S_T}d\vec{r}_T\left(u_z\left(\vec{r}_T\right)e^{id\tilde{k}_N|z_T-z_{N-1}|}\frac{e^{i\tilde{k}r_T}}{r_T}\iiint_{V'}d\vec{r}'\gamma\left(\vec{r}'\right)e^{\left(2id\tilde{k}_1|z_1-z'|\right)-i\tilde{k}\vec{r}'\cdot\left(\frac{\vec{r}_d}{r_d}+\frac{\vec{r}_T}{r_T}\right)}\right) \qquad (2.26)\\
&=\left(-2i\omega\rho_N\right)\left(\frac{\tilde{k}}{4\pi}\right)^2\frac{e^{i\tilde{k}r_d}}{r_d}\Psi\left(\tilde{k},\vec{r}_d\right)\Phi\left(\tilde{k},\vec{r}_d\right),
\end{aligned}$$

where

$$\Psi\left(\tilde{k},\vec{r}_d\right)=\prod_{j=2}^{N-1}\left(T_{j,j-1}T_{j-1,j}e^{2id\tilde{k}_j\left|z_j-z_{j-1}\right|}\right)T_{N,N-1}T_{N-1,N}e^{id\tilde{k}_N\left|z_d-z_{N-1}\right|}$$

$$\Phi\left(\tilde{k},\vec{r}_d\right)=\iint_{S_T}d\vec{r}_T\left(u_z\left(\vec{r}_T\right)e^{id\tilde{k}_N\left|z_T-z_{N-1}\right|}\frac{e^{i\tilde{k}r_T}}{r_T}\iiint_{V'}d\vec{r}\,'\gamma\left(\vec{r}\,'\right)e^{\left(2id\tilde{k}_1\left|z_1-z'\right|\right)-i\tilde{k}\vec{r}\,'\cdot\left(\frac{\vec{r}_d}{r_d}+\frac{\vec{r}_T}{r_T}\right)}\right) \tag{2.27}$$

$$=\iiint_{V'}d\vec{r}\,'\left(\gamma\left(\vec{r}\,'\right)\phi_{inc}\left(\tilde{k},\vec{r}\,'\right)e^{2id\tilde{k}_1\left|z_1-z'\right|-i\tilde{k}\vec{r}\,'\cdot\frac{\vec{r}_d}{r_d}}\right)$$

and

$$\gamma\left(\vec{r}\,'\right)=\gamma_\kappa\left(\vec{r}\,'\right)-\gamma_\rho\left(\vec{r}\,'\right)$$

$$\phi_{inc}\left(\tilde{k},\vec{r}\,'\right)=\iint_{S_T}d\vec{r}_T\left(u_z\left(\vec{r}_T\right)e^{id\tilde{k}_N\left|z_T-z_{N-1}\right|}\frac{e^{i\tilde{k}r_T}}{r_T}e^{-i\tilde{k}\vec{r}\,'\cdot\frac{\vec{r}_T}{r_T}}\right). \tag{2.28}$$

Before continuing the derivation of the scattered field, the analysis needs to be extended to include detectors with finite dimension as opposed to the infinitesimally small point detectors considered thus far. To simplify the analysis, the detector and source transducer will be the same. It will also be assumed that the voltage across the transducer is directly related to the normal particle velocity at the aperture plane according to the relations

$$u_z\left(\vec{r}_T,\omega\right)=K_{uV}\left(\omega\right)V_{inc}\left(\omega\right)G_T\left(\vec{r}_T,\omega\right)H\left(\omega\right)$$

$$V_{refl}\left(\omega\right)=\frac{H\left(\omega\right)}{S_TK_{uV}\left(\omega\right)}\iint_{S_T}d\vec{r}_du_z\left(\vec{r}_d,\omega\right)G_T\left(\vec{r}_d,\omega\right), \tag{2.29}$$

where V_{inc} is the voltage applied to the transducer, V_{refl} is the voltage due to the backscatter, K_{uV} is the conversion constant relating voltage to particle velocity, H is the filtering characteristics for the transducer, and G_T is a gain function that accounts for the focusing of the source (i.e., concavity of the lens) that is defined at the aperture plane. As a result, the total voltage as measured by the transducer is given by

$$V_{refl}\left(\omega\right)=\frac{H\left(\omega\right)}{i\omega\rho_NS_TK_{uV}\left(\omega\right)}\iint_{S_T}d\vec{r}_dG_T\left(\vec{r}_d,\omega\right)\frac{\partial p_s\left(\vec{r}_d\right)}{\partial z_d}$$

$$=\frac{\left(-2\right)\left(\frac{\tilde{k}}{4\pi}\right)^2H\left(\omega\right)}{S_TK_{uV}\left(\omega\right)}\iint_{S_T}d\vec{r}_dG_T\left(\vec{r}_d,\omega\right)\frac{\partial}{\partial z_d}\left(\frac{e^{i\tilde{k}r_d}}{r_d}\Psi\left(\tilde{k},\vec{r}_d\right)\Phi\left(\tilde{k},\vec{r}_d\right)\right)$$

$$\cong \frac{(-2)\left(\frac{\tilde{k}}{4\pi}\right)^2 H(\omega)}{S_T K_{uV}(\omega)} \iiint_{V'} d\vec{r}\,'\gamma(\vec{r}\,')\phi_{inc}\left(\tilde{k},\vec{r}\,'\right)e^{2id\tilde{k}_1|z_1-z'|}\left(\iint_{S_T} d\vec{r}_d G_T(\vec{r}_d,\omega)\Psi\left(\tilde{k},\vec{r}_d\right)\frac{\partial}{\partial z_d}\left(\frac{e^{i\tilde{k}r_d-i\tilde{k}\vec{r}\,'.\frac{\vec{r}_d}{r_d}}}{r_d}\right)\right)$$

$$\cong \frac{(-2i)\left(\frac{\tilde{k}}{4\pi}\right)^2 \tilde{k}H(\omega)}{S_T K_{uV}(\omega)} \iiint_{V'} d\vec{r}\,'\gamma(\vec{r}\,')\phi_{inc}\left(\tilde{k},\vec{r}\,'\right)e^{2id\tilde{k}_1|z_1-z'|}\left(\iint_{S_T} d\vec{r}_d G_T(\vec{r}_d,\omega)\Psi\left(\tilde{k},\vec{r}_d\right)\frac{z_d e^{i\tilde{k}r_d-i\tilde{k}\vec{r}\,'.\frac{\vec{r}_d}{r_d}}}{r_d^2}\right) \tag{2.30}$$

because

$$\frac{\partial r_d}{\partial z_d} = \frac{\partial}{\partial z_d}\left(\sqrt{x_d^2+y_d^2+z_d^2}\right) = \frac{1}{2r_d}\frac{\partial}{\partial z_d}\left(x_d^2+y_d^2+z_d^2\right) = \frac{z_d}{r_d} \tag{2.31}$$

and

$$\frac{\partial}{\partial z_d}\left(|\vec{r}_d-\vec{r}\,'|\right) = \frac{1}{2|\vec{r}_d-\vec{r}\,'|}\frac{\partial}{\partial z_d}\left((x_d-x')^2+(y_d-y')^2+(z_d-z')^2\right) = \frac{(z_d-z')}{|\vec{r}_d-\vec{r}\,'|}, \tag{2.32}$$

yielding

$$\begin{aligned}\frac{\partial}{\partial z_d}\left(\frac{e^{i\tilde{k}r_d-i\tilde{k}\vec{r}\,'.\frac{\vec{r}_d}{r_d}}}{r_d}\right) &= e^{i\tilde{k}|\vec{r}_d-\vec{r}\,'|}\frac{r_d\left(i\tilde{k}\frac{(z_d-z')}{|\vec{r}_d-\vec{r}\,'|}\right)-\frac{z_d}{r_d}}{r_d^2} \cong \frac{z_d}{r_d^3}e^{i\tilde{k}|\vec{r}_d-\vec{r}\,'|}\left(r_d\left(i\tilde{k}\right)-1\right)\\ &\cong \frac{i\tilde{k}z_d}{r_d^2}e^{i\tilde{k}|\vec{r}_d-\vec{r}\,'|} \cong \frac{i\tilde{k}z_d}{r_d^2}e^{i\tilde{k}r_d-i\tilde{k}\vec{r}\,'.\frac{\vec{r}_d}{r_d}}.\end{aligned} \tag{2.33}$$

Regrouping the appropriate terms in Equation (2.30) then yields

$$V_{refl}(\omega) \cong \frac{-2i\tilde{k}^3 V_{inc}(\omega)\Psi_o\left(\tilde{k}\right)\Phi_o\left(\tilde{k}\right)H^2(\omega)}{(4\pi)^2 S_T}, \tag{2.34}$$

where

$$\begin{aligned}\Phi_o\left(\tilde{k}\right) &= \iiint_{V'} d\vec{r}\,'\gamma(\vec{r}\,')W_{source}\left(\tilde{k},\vec{r}\,'\right)\\ W_{source}\left(\tilde{k},\vec{r}\,'\right) &= \left(\iint_{S_T} d\vec{r}_T\left(G_T(\vec{r}_T,\omega)\frac{e^{i\tilde{k}r_T}}{r_T}e^{-i\tilde{k}\vec{r}\,'.\frac{\vec{r}_T}{r_T}}\right)\right)^2 e^{2id\tilde{k}_1|z_1-z'|}\\ \Psi_o\left(\tilde{k}\right) &= \prod_{j=2}^{N-1}\left(T_{j,j-1}T_{j-1,j}e^{2id\tilde{k}_j|z_j-z_{j-1}|}\right)T_{N,N-1}T_{N-1,N}e^{2id\tilde{k}_N|z_T-z_{N-1}|}.\end{aligned} \tag{2.35}$$

Now that the scattered field at the detector location has been found given a known arrangement of scatterers, the analysis needs to be extended for multiple randomly oriented scatterers [*Insana et al.*, 1990]. Because the position of the scatterers is random, the signal at the detector over any given frequency range corresponds to a single realization of a random process whose statistics are related to the properties of the scattering region. In order to see this relationship, consider the second moment of the received voltage given by

$$\begin{aligned} E\left[V_{refl}(\omega)V_{refl}^{*}(\omega)\right] &= \left|\frac{2\tilde{k}^{3}}{(4\pi)^{2}S_{T}}\right|^{2}\left|H(\omega)\right|^{4}\left|\Psi_{o}(\tilde{k})\right|^{2}\left|V_{inc}(\omega)\right|^{2}E\left[\left|\Phi_{o}(\tilde{k})\right|^{2}\right] \\ &= \left|\frac{2\tilde{k}^{3}}{(4\pi)^{2}S_{T}}\right|^{2}\left|H(\omega)\right|^{4}\left|\Psi_{o}(\tilde{k})\right|^{2}\left|V_{inc}(\omega)\right|^{2}\iiint_{V'}d\vec{r}'\left(\iiint_{V'}d\vec{r}''\begin{pmatrix}W_{source}(\tilde{k},\vec{r}')W_{source}^{*}(\tilde{k},\vec{r}'')\\ E\left[\gamma(\vec{r}')\gamma(\vec{r}'')\right]\end{pmatrix}\right), \end{aligned} \tag{2.36}$$

where '*' is the complex conjugate and $E[\sim]$ denotes expected value [*Peebles*, 1993].

In order to simplify Equation (2.36), the W_{source} terms need to be simplified. Hence, assume that the velocity potential field in the scattering region corresponds to a focused Gaussian beam given by

$$\begin{aligned} \iint_{S_T}d\vec{r}_T\left(u_z(\vec{r}_T)\frac{e^{i\tilde{k}r_T - i\tilde{k}\vec{r}'\cdot\frac{\vec{r}_T}{r_T}}}{r_T}\right) &\cong \left(G_o u_z(0,0,z_T)e^{-\left(\left(\frac{x'}{w_x}\right)^2+\left(\frac{y'}{w_y}\right)^2+\left(\frac{z'}{w_z}\right)^2\right)}\right)e^{i\tilde{k}|\hat{z}z_T-\vec{r}'|} \\ &\cong \left(G_o u_z(0,0,z_T)e^{-\left(\left(\frac{x'}{w_x}\right)^2+\left(\frac{y'}{w_y}\right)^2+\left(\frac{z'}{w_z}\right)^2\right)}\right)e^{i\tilde{k}(z_T-\hat{z}\cdot\vec{r}')}, \end{aligned} \tag{2.37}$$

where w_x, w_y, and w_z set the width of the focal region along the respective coordinate axes, G_o is the focusing gain for the transducer, and $u_z(0,0,z_T)$ is the particle velocity at the center of the aperture plane for the transducer. A similar assumption was shown to be valid in the focal plane, i.e., z'=0, by *Barber* [1991]. For a spherically focused transducer, these quantities are approximately given by [*Kino*, 1987; *Barber*, 1991]

$$G_o = \frac{a^2}{2F} \tag{2.38}$$

and

$$w_x = w_y = \frac{0.51\sqrt{2}\lambda f\#}{\sqrt{\ln(2)}} = 0.87\lambda f\# \quad w_z = \frac{3.54\sqrt{2}\lambda(f\#)^2}{\sqrt{\ln(2)}} = 6.01\lambda(f\#)^2 \tag{2.39}$$

after matching the ideal –3-dB transmit beamwidths and depth of focus (i.e., $1.02\lambda f\#$ and $7.08\lambda f\#^2$) [*Kino*, 1987] to the corresponding Gaussian beamwidths and depth of focus. In these equations, a is the radius of the transducer aperture, F is the focal length for the transducer, λ is the wavelength, and $f\#$ is the f-number for the transducer (i.e., focal length over aperture diameter).

Although *Barber* [1991] showed that the $w_{x,y}$ equation is a good approximation to the real beamwidth for the ideal transducer, the equation for w_z had not been validated. Hence, the equation for w_z was also tested by calculating the axial field intensity using equations given by *Kino* [1987] for sources with f-numbers of 1, 2, and 4, a diameter of 2 cm, for frequencies in the range of 7 to 10 MHz. The equivalent Gaussian depth of field w_z for each case was then found by fitting the calculated field intensity directly to a Gaussian distribution. The w_z found by the Gaussian fit always differed by less than 4.4 % from the w_z calculated using Equation (2.39). An example axial field and its equivalent Gaussian fit are shown in Figure 2.2. A more detailed comparison of the Gaussian approximation to the real field intensity for a focused source is found in Appendix E.

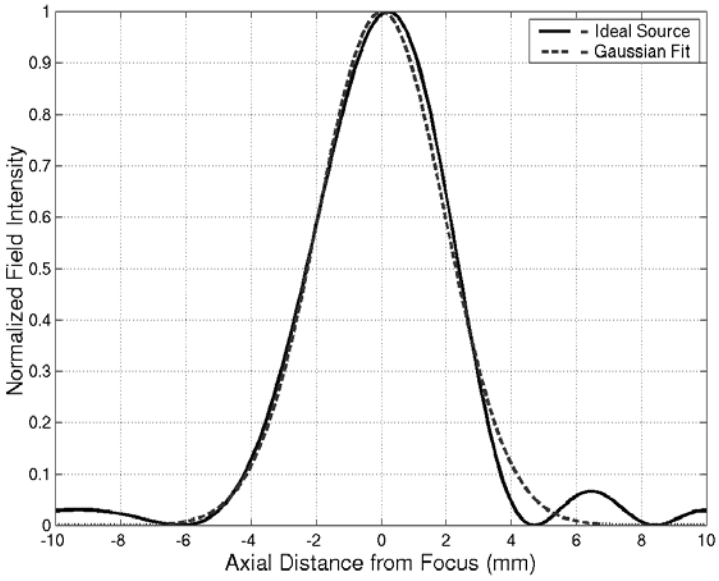

Figure 2.2: Example ideal axial intensity field and Gaussian fit found for a spherically focused *f*/2 transducer at a frequency of 9 MHz.

Based on the approximation in Equation (2.37), W_{source} simplifies to yield

$$W_{source}\left(\tilde{k},\vec{r}\,'\right) \cong \left(G_o e^{-\left(\left(\frac{x'}{w_x}\right)^2+\left(\frac{y'}{w_y}\right)^2+\left(\frac{z'}{w_z}\right)^2\right)} \right)^2 e^{i2\tilde{k}\left(z_T-z'\right)} e^{2id\tilde{k}_1\left|z_1-z'\right|}$$
$$= \hat{W}_{source}\left(\vec{r}\,'\right) e^{i2\tilde{k}z_T} e^{-i2\tilde{k}z'} e^{2id\tilde{k}_1\left|z_1-z'\right|}. \tag{2.40}$$

Substituting Equation (2.40) into Equation (2.36) then yields

$$E\left[\left|V_{refl}\right|^2\right] = \left|\frac{2\tilde{k}^3}{\left(4\pi\right)^2 S_T}\right|^2 \left|H(\omega)\right|^4 \left|\Psi_o\left(\tilde{k}\right)\right|^2 \left|V_{inc}(\omega)\right|^2 e^{-4\alpha z_T} \iiint_{V'} d\vec{r}\,' \iiint_{V'} d\vec{r}\,'' \begin{pmatrix} \hat{W}_{source}\left(\vec{r}\,'\right)\hat{W}^*_{source}\left(\vec{r}\,''\right) \\ E\left[\gamma\left(\vec{r}\,'\right)\gamma\left(\vec{r}\,''\right)\right] \\ e^{-i2k_1\hat{z}\cdot\left(\vec{r}\,'-\vec{r}\,''\right)} e^{2\alpha_1\hat{z}\cdot\left(\vec{r}\,'+\vec{r}\,''\right)} \end{pmatrix}. \tag{2.41}$$

Now perform a change of variables by letting $\Delta\vec{r} = \vec{r}\,' - \vec{r}\,''$ and $\vec{s} = \left(\vec{r}\,' + \vec{r}\,''\right)/2$. The $\hat{W}_{source}\left(\vec{r}\,'\right)\hat{W}_{source}\left(\vec{r}\,''\right)$ term in Equation (2.41) then becomes

$$\hat{W}_{source}\left(\vec{r}\,'\right)\hat{W}_{source}\left(\vec{r}\,''\right) = G_o^4 e^{-2\left(\left(\frac{x'^2+x''^2}{w_x^2}\right)+\left(\frac{y'^2+y''^2}{w_y^2}\right)+\left(\frac{z'^2+z''^2}{w_z^2}\right)\right)}$$
$$= G_o^4 e^{-4\left(\left(\frac{s_x^2}{w_x^2}\right)+\left(\frac{s_y^2}{w_y^2}\right)+\left(\frac{s_z^2}{w_z^2}\right)\right)} e^{-\left(\left(\frac{\Delta r_x^2}{w_x^2}\right)+\left(\frac{\Delta r_y^2}{w_y^2}\right)+\left(\frac{\Delta r_z^2}{w_z^2}\right)\right)}. \tag{2.42}$$

Allowing Equation (2.41) to be written as

$$E\left[\left|V_{refl}\right|^2\right] = \frac{G_o^4\left|2\tilde{k}^3\right|^2 \left|H(\omega)\right|^4 \left|\Psi_o\left(\tilde{k}\right)\right|^2 \left|V_{inc}(\omega)\right|^2}{\left|\left(4\pi\right)^2 S_T\right|^2} e^{-4\alpha z_T}$$
$$\iiint_{V'} d\Delta\vec{r} \left(\iiint_{V'} d\vec{s} \begin{pmatrix} e^{-4\left(\left(\frac{s_x^2}{w_x^2}\right)+\left(\frac{s_y^2}{w_y^2}\right)+\left(\frac{s_z^2}{w_z^2}\right)\right)} e^{-\left(\left(\frac{\Delta r_x^2}{w_x^2}\right)+\left(\frac{\Delta r_y^2}{w_y^2}\right)+\left(\frac{\Delta r_z^2}{w_z^2}\right)\right)} \\ E\left[\gamma\left(\vec{s}+\frac{\Delta\vec{r}}{2}\right)\gamma\left(\vec{s}-\frac{\Delta\vec{r}}{2}\right)\right] e^{-i2k_1\hat{z}\cdot\left(\Delta\vec{r}\right)} e^{4\alpha_1\hat{z}\cdot\vec{s}} \end{pmatrix} \right) \tag{2.43}$$
$$= \frac{G_o^4\left|2\tilde{k}^3\right|^2 \left|H(\omega)\right|^4 \left|\Psi_o\left(\tilde{k}\right)\right|^2 \left|V_{inc}(\omega)\right|^2}{\left|\left(4\pi\right)^2 S_T\right|^2} e^{-4\alpha z_T} \iiint_{V'} d\Delta\vec{r} \left(B_\gamma\left(\Delta\vec{r}\right) e^{-\left(\left(\frac{\Delta r_x^2}{w_x^2}\right)+\left(\frac{\Delta r_y^2}{w_y^2}\right)+\left(\frac{\Delta r_z^2}{w_z^2}\right)\right)} e^{-i2k_1\hat{z}\cdot\left(\Delta\vec{r}\right)} \right),$$

where

$$B_\gamma\left(\Delta\vec{r}\right) = \iiint_{V'} d\vec{s} \left(E\left[\gamma\left(\vec{s}+\frac{\Delta\vec{r}}{2}\right)\gamma\left(\vec{s}-\frac{\Delta\vec{r}}{2}\right)\right] e^{-4\left(\left(\frac{s_x^2}{w_x^2}\right)+\left(\frac{s_y^2}{w_y^2}\right)+\left(\frac{s_z^2}{w_z^2}\right)\right)} e^{4\alpha_1\hat{z}\cdot\vec{s}} \right). \tag{2.44}$$

Assuming that γ is weakly stationary within the scattering volume, the autocorrelation function $E\left[\gamma\left(\vec{u}+\frac{\Delta\vec{r}}{2}\right)\gamma\left(\vec{u}-\frac{\Delta\vec{r}}{2}\right)\right]$ depends only on the separation between the points being correlated, $\Delta\vec{r}$ [*Insana et al.*, 1990]. Hence, Equation (2.44) simplifies to

$$\begin{aligned} B_\gamma(\Delta\vec{r}) &= R_{\gamma\gamma}(\Delta\vec{r})\iiint_{V'} d\vec{s}\left(e^{-4\left(\left(\frac{s_x^2}{w_x^2}\right)+\left(\frac{s_y^2}{w_y^2}\right)+\left(\frac{s_z^2}{w_z^2}\right)\right)}e^{4\alpha_1\hat{z}\cdot\vec{s}}\right) \\ &= R_{\gamma\gamma}(\Delta\vec{r})\left(\frac{w_x\sqrt{\pi}}{2}\right)\left(\frac{w_y\sqrt{\pi}}{2}\right)\left(\frac{w_z\sqrt{\pi}}{2}e^{\alpha_1^2 w_z^2}\right) \\ &= R_{\gamma\gamma}(\Delta\vec{r})\left(\frac{w_x w_y w_z \pi^{\frac{3}{2}}}{8}\right)e^{\alpha_1^2 w_z^2}, \end{aligned} \tag{2.45}$$

where $R_{\gamma\gamma}$ is the autocorrelation function.

Now that the innermost integral in Equation (2.43) has been solved, we can proceed to evaluate the integral over $d\Delta\vec{r}$ in Equation (2.43) as well. Substituting Equation (2.45) and the expression for Ψ_o given in Equation (2.35) back into Equation (2.43) yields

$$\begin{aligned} E\left[\left|V_{refl}\right|^2\right] = {} & \frac{4T_o^2 G_o^4 \left|\tilde{k}\right|^6 \left|V_{inc}(\omega)\right|^2 \left|H(\omega)\right|^4}{(4\pi)^4 S_T^2}\left(\frac{w_x w_y w_z \pi^{\frac{3}{2}}}{8}\right)e^{\alpha_1^2 w_z^2}e^{-4\alpha_{tot}z_T} \\ & \iiint_{V'} d\Delta\vec{r}\left(R_{\gamma\gamma}(\Delta\vec{r})e^{-\left(\left(\frac{\Delta r_x^2}{w_x^2}\right)+\left(\frac{\Delta r_y^2}{w_y^2}\right)+\left(\frac{\Delta r_z^2}{w_z^2}\right)\right)}e^{-i2k_1\hat{z}\cdot(\Delta\vec{r})}\right), \end{aligned} \tag{2.46}$$

where

$$\begin{aligned} T_o &= \prod_{j=2}^{N}\left(T_{j,j-1}T_{j-1,j}\right) \\ \alpha_{tot} &= \alpha = \left(\alpha + \left(\sum_{j=2}^{N-1} d\alpha_j \left|z_j - z_{j-1}\right|\right) + d\alpha_N \left|z_T - z_{N-1}\right|\right). \end{aligned} \tag{2.47}$$

The total attenuation (attenuation along the entire propagation path) is α in this case because it was already assumed that $\tilde{k}$ was a weighted average of the wavenumbers for the different layers. Because the location of the scatterers in the scattering region is random, the autocorrelation function will be zero except for separations $\Delta\vec{r}$ smaller than the size of the scatterers. Also,

because the scatterers are typically much smaller than the focal dimensions (i.e., subresolution scatterers), $e^{-\left(\left(\frac{\Delta r_x^2}{w_x^2}\right)+\left(\frac{\Delta r_y^2}{w_y^2}\right)+\left(\frac{\Delta r_z^2}{w_z^2}\right)\right)} \approx 1$. In addition, the limits of the integration over $d\Delta\vec{r}$ can be extended to infinity yielding

$$E\left[\left|V_{refl}\right|^2\right] = \frac{4T_o^2 G_o^4 \left|\tilde{k}\right|^6 \left|V_{inc}(\omega)\right|^2 \left|H(\omega)\right|^4}{(4\pi)^4 S_T^2} \left(\frac{w_x w_y w_z \pi^{\frac{3}{2}}}{8}\right) e^{\alpha_1^2 w_z^2} e^{-4\alpha z_T} \Re_{\gamma\gamma}(2k_1\hat{z}), \qquad (2.48)$$

where $\Re_{\gamma\gamma}$ is the Fourier transform of $R_{\gamma\gamma}$, (i.e., the power spectral density function).

Before proceeding with the analysis, consider the effects of windowing on the received signal. Often when estimating the tissue properties, the backscattered data are windowed to improve the spatial resolution of the estimated tissue microstructure. The effect of windowing is twofold. First, the windowing in the time domain results in blurring of the spectrum in the frequency domain due to the associated convolution. It may be possible to avoid this blurring by employing a modeling approach, such as autoregressive modeling, on some finite data set to obtain a local estimate for the scattered spectrum rather than performing direct windowing followed by the FFT operation [*Kay and Marple*, 1981]. The blurring effect can also be compensated for using a Gaussian model and subsequent Gaussian transformation as will be discussed in Chapter 5.

The second effect of windowing is to decrease the size of the scattering region along the z-axis. As a result, the integral in Equation (2.44) needs to be reevaluated yielding

$$\begin{aligned} B_\gamma(\Delta\vec{r}) &= R_{\gamma\gamma}(\Delta\vec{r}) \iiint_{V'} d\vec{s} \left(e^{-4\left(\left(\frac{s_x^2}{w_x^2}\right)+\left(\frac{s_y^2}{w_y^2}\right)+\left(\frac{s_z^2}{w_z^2}\right)\right)} e^{4\alpha_1 \hat{z}\cdot\vec{s}} \right) \\ &= R_{\gamma\gamma}(\Delta\vec{r}) \left(\frac{w_x\sqrt{\pi}}{2}\right)\left(\frac{w_y\sqrt{\pi}}{2}\right) \int_{-L/2}^{L/2} ds_z \left(g_{win}(s_z) e^{-\frac{4s_z^2}{w_z^2}} e^{4\alpha_1 s_z} \right), \end{aligned} \qquad (2.49)$$

where L is the length of the window centered at the focus (i.e., the time gate T_{win} is given by $T_{win} = 2L/c$), and g_{win} is the amplitude weighting function corresponding to the desired window. In general, this integral cannot be evaluated in closed form. Substituting Equation (2.49) back into Equation (2.43) and assuming that the scatterers are small compared to L yields the new expected spectrum given by

$$E\left[\left|V_{refl}\right|^2\right] = \frac{T_o^2 G_o^4 \left|\tilde{k}\right|^6 \left|V_{inc}(\omega)\right|^2 \left|H(\omega)\right|^4}{(4\pi)^3 S_T^2 A_{comp}(\omega)} \left(\frac{w_x w_y}{4}\right) \Re_{\gamma\gamma}(2k_1\hat{z}), \tag{2.50}$$

where

$$A_{comp} = \frac{e^{4\alpha z_T}}{\int_{-L/2}^{L/2} ds_z \left(g_{win}(s_z) e^{-\frac{4s_z^2}{w_z^2}} e^{4\alpha_1 s_z} \right)}. \tag{2.51}$$

If w_z goes to infinity and g_{win} is a rectangular windowing function, the integral reduces to

$$A_{OM}(\omega) = \frac{4\alpha_1 \, \mathrm{e}^{4\alpha z_T}}{\mathrm{e}^{4\alpha_1 \frac{L}{2}} - \mathrm{e}^{-4\alpha_1 \frac{L}{2}}}, \tag{2.52}$$

which is just the O'Donnell and Miller attenuation-compensation function [*O'Donnell and Miller*, 1981]. Hence, Equation (2.51) is a more general attenuation-compensation function that corrects for focusing, windowing, and attenuation.

Upon comparing Equation (2.52) to Equation (2.51), it is clear that the O'Donnell-Miller attenuation-compensation function neglects the natural falloff of the field, increasing the evaluation of the integral in Equation (2.51) and subsequently undercompensating for the attenuation. As a result, O'Donnell-Miller compensation should result in an overestimate of the scatterer size for focused sources because the values at higher frequencies are smaller than they should be due to uncompensated attenuation. Likewise, if we neglect all field variations in the scattering region, Equation (2.51) becomes

$$A_{PC}(\omega) = \frac{\mathrm{e}^{4\alpha z_T}}{L}, \tag{2.53}$$

which is point compensation [*Oelze and O'Brien*, 2002a]. Point compensation will either underestimate or overestimate the scatterer size depending upon the relative importance of diffraction (w_z term) and attenuation (α_1 term) due to the sign difference in the integrand of Equation (2.51).

In the above development, the windowing function was centered about the focus, and although this is the conventional method employed for quantitative ultrasound imaging, errors in the assumed sound speed for the tissue can lead to shifts of the window away from the focus (i.e., offset window by a distance z_o). As a result, variations in the expected backscatter with

window location are of interest. The only change in the above development is that the integral in the attenuation-compensation function becomes

$$\begin{aligned}\int_{z_o-L/2}^{z_o+L/2} ds_z \left(g_{win}(s_z - z_o) e^{-\frac{4s_z^2}{w_z^2}} e^{4\alpha_1 s_z} \right) &= \int_{-L/2}^{L/2} ds_z' \left(g_{win}(s_z') e^{-\frac{4(s_z'+z_o)^2}{w_z^2}} e^{4\alpha_1 (s_z'+z_o)} \right) \\ &= e^{4\alpha_1 z_o} e^{-\frac{4z_o^2}{w_z^2}} \int_{-L/2}^{L/2} ds_z' \left(g_{win}(s_z') e^{-\frac{4s_z'^2}{w_z^2}} e^{\left(4\alpha_1 - \frac{8z_o}{w_z^2}\right) s_z'} \right),\end{aligned} \tag{2.54}$$

yielding a new attenuation-compensation function given by

$$A_{comp} = \frac{e^{4\alpha z_T} e^{-4\alpha_1 z_o + \frac{4z_o^2}{w_z^2}}}{\int_{-L/2}^{L/2} ds_z' \left(g_{win}(s_z') e^{-\frac{4s_z'^2}{w_z^2}} e^{\left(4\alpha_1 - \frac{8z_o}{w_z^2}\right) s_z'} \right)}. \tag{2.55}$$

From Equation (2.50), it is clear that the expected value of the scattered intensity for some frequency $\tilde{k}$ is directly related to the correlation properties of the scatterers in the medium. All that remains is to relate the correlation properties to the physical structure of the tissue. Let us assume that the medium consists only of scatterers of a single size and geometry. In this case, the autocorrelation function $R_{\gamma\gamma}$ becomes

$$R_{\gamma\gamma}(\Delta\vec{r}) = \bar{n} V_s \gamma_o^2 b_\gamma(\Delta\vec{r}), \tag{2.56}$$

where $\bar{n}$ is the average number of scatterers per unit volume, V_s is the average volume of a single scatterer, and γ_o^2 is the mean-square variation in the acoustic impedance per particle [*Insana et al.*, 1990]. The function b_γ is the correlation function dependent on the scatterer geometry.

In the literature, b_γ and hence the power spectral density functions have been evaluated for many different scatterer geometries [*Insana et al.*, 1990]. However, the most common types are the spherical shell model applicable to the glass microsphere phantoms commonly used to evaluate the backscattering theory and the Gaussian model that is often assumed to capture the scattering behavior of tissue. The correlation functions and resulting power spectral density functions for each of these cases are given by [*Insana et al.*, 1990]

$$
\begin{aligned}
b_{\gamma\_ss}\left(\Delta\vec{r}\right) &= \begin{cases} \dfrac{a_{eff}\left|\Delta\vec{r}\right|}{6} & \dfrac{\left|\Delta\vec{r}\right|}{2a_{eff}} \le 1 \quad (Spherical \quad Shell) \\ 0 \quad else \end{cases} \\
\Re_{\gamma\gamma\_ss}\left(2k\hat{z}\right) &= \bar{n}V_s^2\gamma_o^2\left[j_o\left(2ka_{eff}\right)\right]^2 \quad (Spherical \quad Shell) \\
b_{\gamma\_G}\left(\Delta\vec{r}\right) &= e^{-\frac{\left|\Delta\vec{r}\right|^2}{0.827a_{eff}^2}} \quad (Gaussian) \\
\Re_{\gamma\gamma\_G}\left(2k\hat{z}\right) &= \bar{n}V_s^2\gamma_o^2 e^{-.827k^2a_{eff}^2}. \quad (Gaussian)
\end{aligned}
\tag{2.57}
$$

In these equations, a_{eff} is the effective radius of the scatterer, and j_0 is the 0th-order spherical Bessel function of the first kind.

In the derivation of Equations (2.50) and (2.51), it was assumed that the transmit and receive foci were at the same location. In clinical arrays, however, the two foci often occur at different locations due to the small number of foci used on transmit. When the two foci are at different locations, Equation (2.40) becomes

$$
\begin{aligned}
W_{source}\left(\tilde{k},\vec{r}\,'\right) \cong & \left(G_o e^{-\left(\left(\frac{x'}{w_x}\right)^2+\left(\frac{y'}{w_y}\right)^2+\left(\frac{z'}{w_z}\right)^2\right)} \right) \\
& \left(G_{o\_trans} e^{-\left(\left(\frac{x'}{w_{x\_trans}}\right)^2+\left(\frac{y'}{w_{y\_trans}}\right)^2+\left(\frac{z'-z_{trans}}{w_{z\_trans}}\right)^2\right)} \right) e^{i2\tilde{k}\left(z_T-z'\right)} e^{2id\tilde{k}_1\left|z_1-z'\right|}.
\end{aligned}
\tag{2.58}
$$

As a result, Equation (2.36) becomes

$$
\begin{aligned}
E\left[\left|V_{refl}(\omega)\right|^2\right] &= \left|\frac{2\tilde{k}^3}{(4\pi)^2 S_T}\right|^2 T_o^2\left|H(\omega)\right|^4\left|V_{inc}(\omega)\right|^2 \iiint_{V'} d\vec{r}\,' \left(\iiint_{V'} d\vec{r}\,'' \begin{pmatrix} W_{source}\left(\tilde{k},\vec{r}\,'\right)W_{source}^*\left(\tilde{k},\vec{r}\,''\right) \\ E\left[\gamma\left(\vec{r}\,'\right)\gamma\left(\vec{r}\,''\right)\right] \end{pmatrix} \right) \\
&= G_{o\_trans}^2 G_o^2 T_o^2 \left|\frac{2\tilde{k}^3}{(4\pi)^2 S_T}\right|^2 \left|H(\omega)\right|^4\left|V_{inc}(\omega)\right|^2 e^{-4\alpha z_T} \\
&\quad \iiint_{V'} d\vec{r}\,' \left(\iiint_{V'} d\vec{r}\,'' \begin{pmatrix} E\left[\gamma\left(\vec{r}\,'\right)\gamma\left(\vec{r}\,''\right)\right] e^{-2ik_1\left(z'-z''\right)+2\alpha_1\left(z'+z''\right)} e^{-\left(\left(\frac{x'^2+x''^2}{w_x^2}\right)+\left(\frac{y'^2+y''^2}{w_y^2}\right)+\left(\frac{z'^2+z''^2}{w_z^2}\right)\right)} \\ e^{-\left(\left(\frac{x'^2+x''^2}{w_{x\_trans}^2}\right)+\left(\frac{y'^2+y''^2}{w_{y\_trans}^2}\right)+\left(\frac{\left(z'-z_{trans}\right)^2+\left(z''-z_{trans}\right)^2}{w_{z\_trans}^2}\right)\right)} \end{pmatrix} \right),
\end{aligned}
\tag{2.59}
$$

and Equations (2.43) and (2.44) become

$$E\left[\left|V_{refl}(\omega)\right|^2\right] = 4G_{o\_trans}^2 G_o^2 T_o^2 \left|\frac{\widetilde{k}}{S_T}\right|^2 \left|\frac{\widetilde{k}}{4\pi}\right|^4 \left|H(\omega)\right|^4 \left|V_{inc}(\omega)\right|^2 e^{-4\alpha z_T} \iiint_{V'} d\Delta\vec{r} \begin{pmatrix} e^{-\frac{1}{2}\left(\frac{\Delta x^2}{w_x^2}+\frac{\Delta x^2}{w_{x\_trans}^2}+\frac{\Delta y^2}{w_y^2}+\frac{\Delta y^2}{w_{y\_trans}^2}+\frac{\Delta z^2}{w_z^2}+\frac{\Delta z^2}{w_{z\_trans}^2}\right)} \\ e^{-2k_1\Delta r_z} B_\gamma(\Delta\vec{r}) \end{pmatrix}, \tag{2.60}$$

and

$$B_\gamma(\Delta\vec{r}) = \iiint_{V'} d\vec{s} \left(g_{win}(s_z) E\left[\gamma\left(\vec{s}+\frac{\Delta\vec{r}}{2}\right)\gamma\left(\vec{s}-\frac{\Delta\vec{r}}{2}\right)\right] e^{-2\left(\frac{s_x^2}{w_x^2}+\frac{s_x^2}{w_{x\_trans}^2}+\frac{s_y^2}{w_y^2}+\frac{s_y^2}{w_{y\_trans}^2}+\frac{s_z^2}{w_z^2}+\frac{(s_z-z_{trans})^2}{w_{z\_trans}^2}\right)} e^{4\alpha_1 s_z} \right), \tag{2.61}$$

which after making the same approximations regarding the field and scatterers can be written as

$$E\left[\left|V_{refl}(\omega)\right|^2\right] \cong 4G_{o\_trans}^2 G_o^2 T_o^2 \left|\frac{\widetilde{k}}{S_T}\right|^2 \left|\frac{\widetilde{k}}{4\pi}\right|^4 \left|H(\omega)\right|^4 \left|V_{inc}(\omega)\right|^2 e^{-4\alpha z_T} \Re_{\gamma\gamma}(2k_1\hat{z}) B_\gamma, \tag{2.62}$$

where

$$\begin{aligned} B_\gamma &= \iiint_{V'} d\vec{s} \left(g_{win}(s_z) e^{-2\left(\frac{s_x^2}{w_x^2}+\frac{s_x^2}{w_{x\_trans}^2}+\frac{s_y^2}{w_y^2}+\frac{s_y^2}{w_{y\_trans}^2}+\frac{s_z^2}{w_z^2}+\frac{(s_z-z_{trans})^2}{w_{z\_trans}^2}\right)} e^{4\alpha_1 s_z} \right) \\ &= \frac{\sqrt{\pi}}{\sqrt{2\left(\frac{1}{w_x^2}+\frac{1}{w_{x\_trans}^2}\right)}} \frac{\sqrt{\pi}}{\sqrt{2\left(\frac{1}{w_y^2}+\frac{1}{w_{y\_trans}^2}\right)}} \int_{-L/2}^{L/2} ds_z g_{win}(s_z) e^{-2\left(\frac{s_z^2}{w_z^2}+\frac{(s_z-z_{trans})^2}{w_{z\_trans}^2}\right)+4\alpha_1 s_z} \\ &= \frac{\pi w_x w_{x\_trans} w_y w_{y\_trans}}{2\sqrt{\left(w_{x\_trans}^2+w_x^2\right)\left(w_{y\_trans}^2+w_y^2\right)}} \int_{-L/2}^{L/2} ds_z g_{win}(s_z) e^{-2\left(\frac{s_z^2}{w_z^2}+\frac{(s_z-z_{trans})^2}{w_{z\_trans}^2}\right)+4\alpha_1 s_z}. \end{aligned} \tag{2.63}$$

Hence, the expected backscattered voltage power spectrum for the case when the transmit and receive foci are at different locations would be given by

$$\mathrm{E}\left[\left|V_{refl}(\omega)\right|^2\right] = \frac{G_{o\_trans}^2 G_o^2 T_o^2 \left|\widetilde{k}\right|^6 \left|H(\omega)\right|^4 \left|V_{inc}(\omega)\right|^2}{2(4\pi)^3 S_T^2 A_{comp}(\omega)} \left(\frac{w_x w_{x\_trans} w_y w_{y\_trans}}{\sqrt{\left(w_{x\_trans}^2+w_x^2\right)\left(w_{y\_trans}^2+w_y^2\right)}} \right) \Re_{\gamma\gamma}(2k_1\hat{z}), \tag{2.64}$$

where

$$A_{comp}(\omega) = \frac{\mathrm{e}^{4\alpha z_T}}{\left(\int_{-L/2}^{L/2} ds_z g_{win}(s_z) \mathrm{e}^{-2\left(\frac{s_z^2}{w_z^2}+\frac{(s_z-z_{trans})^2}{w_{z\_trans}^2}\right)+4\alpha_1 s_z} \right)}. \tag{2.65}$$

2.2 Traditional Method to Obtain Scatterer Size

Before concluding the discussion on the theoretical model for estimating scatterer size, it is useful to review the traditional method for obtaining the size estimate. In order to obtain the size estimate, certain calibrations need to be performed to isolate the tissue correlation term $\Re_{\gamma\gamma}$ from Equation (2.51). First, the source filtering terms can be removed by dividing by a reference spectrum. Normally, the scattered signal reflected off of a rigid plane positioned parallel to the focal plane is used as the reference [*Madsen et al.*, 1984*; Lizzi et al.*, 1983; *Insana et al.*, 1990], but signal from a well characterized tissue mimicking phantom may also be used [*Gerig et al.*, 2003].

We can solve for the returned voltage from a rigid plane placed parallel to the focal plane by treating the reflected field from the plane as a virtual source. Hence, the reflected field at the aperture of the transducer is given by

$$p_{plane}\left(\vec{r}_d,\omega\right) = -2i\omega\rho_o \iint_{S_f} d\vec{r}_f u_z\left(\vec{r}_f\right)\frac{e^{ik_o r_d}}{4\pi r_d} e^{-ik_o \frac{\vec{r}_d}{r_d}\cdot\vec{r}_f}, \tag{2.66}$$

where S_f is the surface of the rigid plane placed near the focus and

$$u_z\left(\vec{r}_f\right) = \frac{-2ik_o K_{uV}(\omega)V_{inc}(\omega)H(\omega)}{4\pi}\iint_{S_T} d\vec{r}_T G_T\left(\vec{r}_T,\omega\right)\frac{e^{ik_o r_T - ik_o \vec{r}_f\cdot\frac{\vec{r}_T}{r_T}}}{r_T}. \tag{2.67}$$

As a result, the returned voltage detected by the source is given by

$$V_{plane}(\omega) = \frac{H(\omega)}{i\omega\rho_o S_T K_{uV}(\omega)}\iint_{S_T} d\vec{r}_d G_T\left(\vec{r}_d,\omega\right)\frac{\partial p_{plane}}{\partial z_d}. \tag{2.68}$$

The derivative of p_{plane} is given by

$$\frac{\partial}{\partial z_d} p_{plane}\left(\vec{r}_d,\omega\right) = \frac{-2i\omega\rho_o}{4\pi}\iint_{S_f} d\vec{r}_f u_z\left(\vec{r}_f\right)\frac{\partial}{\partial z_d}\left(\frac{e^{ik_o r_d} e^{-ik_o \frac{\vec{r}_d}{r_d}\cdot\vec{r}_f}}{r_d}\right)$$

$$\Rightarrow \frac{\partial}{\partial z_d}\left(\frac{e^{ik_o r_d - ik_o \vec{r}_f\cdot\frac{\vec{r}_d}{r_d}}}{r_d}\right) \cong \frac{ik_o}{r_d} e^{ik_o r_d - ik_o \vec{r}_f\cdot\frac{\vec{r}_d}{r_d}} \tag{2.69}$$

$$\Rightarrow \frac{\partial}{\partial z_d} p_{plane}\left(\vec{r}_d,\omega\right) = \frac{2\omega\rho_o k_o}{4\pi}\iint\limits_{S_f} d\vec{r}_f u_z\left(\vec{r}_f\right)\frac{e^{ik_o r_d - ik_o \vec{r}_f\cdot\frac{\vec{r}_d}{r_d}}}{r_d}.$$

Hence,

$$\begin{aligned} V_{plane}(\omega) &= \frac{-4k_o^2 V_{inc}(\omega)H^2(\omega)}{S_T(4\pi)^2}\iint\limits_{S_T} d\vec{r}_d G_T\left(\vec{r}_d,\omega\right)\left(\iint\limits_{S_f} d\vec{r}_f \frac{e^{ik_o r_d - ik_o \vec{r}_f\cdot\frac{\vec{r}_d}{r_d}}}{r_d}\left(\iint\limits_{S_T} d\vec{r}_T G_T\left(\vec{r}_T,\omega\right)\frac{e^{ik_o r_T - ik_o \vec{r}_f\cdot\frac{\vec{r}_T}{r_T}}}{r_T}\right)\right) \\ &= \frac{-4k_o^2 V_{inc}(\omega)H^2(\omega)}{S_T(4\pi)^2}\iint\limits_{S_f} d\vec{r}_f\left(\iint\limits_{S_T} d\vec{r}_d G_T\left(\vec{r}_d,\omega\right)\frac{e^{ik_o r_d - ik_o \vec{r}_f\cdot\frac{\vec{r}_d}{r_d}}}{r_d}\right)^2. \end{aligned} \tag{2.70}$$

Likewise, if it is assumed once again that the velocity potential fields near the focus are approximately Gaussian, then Equation (2.70) becomes

$$\begin{aligned} V_{plane}(\omega) &= \frac{-4k_o^2 G_o^2 V_{inc}(\omega)H^2(\omega)}{S_T(4\pi)^2} e^{i2k_o\left(z_T - z_f\right)} e^{-2\left(\frac{z_f}{w_z}\right)^2}\iint\limits_{S_f} d\vec{r}_f e^{-2\left(\frac{x_f}{w_x}\right)^2 - 2\left(\frac{y_f}{w_y}\right)^2} \\ &= \frac{-w_x w_y k_o^2 G_o^2 V_{inc}(\omega)H^2(\omega)}{8\pi S_T} e^{i2k_o\left(z_T - z_f\right)} e^{-2\left(\frac{z_f}{w_z}\right)^2}. \end{aligned} \tag{2.71}$$

Hence, the magnitude of the voltage returned from the rigid plane placed at the focal plane $z_f = 0$ at a particular frequency is proportional to

$$\begin{aligned} \left|V_{plane}(\omega)\right| &\propto \left|V_{inc}(\omega)\right|\left|H(\omega)\right|^2 \\ \Rightarrow \left|V_{plane}(\omega)\right|^2 &\propto \left|V_{inc}(\omega)\right|^2\left|H(\omega)\right|^4, \end{aligned} \tag{2.72}$$

where the loss of the k_o^2 dependence in the proportionality results from both w_x and w_y being proportional to λ.

Based on Equation (2.72), Equation (2.51) can be rewritten as a proportionality as

$$E\left[\left|V_{refl}\right|^2\right] \propto k_o^4\left|V_{plate}(\omega)\right|^2 \frac{F_\gamma\left(f,a_{eff}\right)}{A_{comp}(\omega)}, \tag{2.73}$$

where

$$F_\gamma\left(f,a_{eff}\right) = \frac{\Re_{\gamma\gamma}\left(2k_1\hat{z}\right)}{\bar{n}V_s^2\gamma_o^2} \tag{2.74}$$

and is called the form factor for the medium [*Insana et al.*, 1990]. The scatterer size can then be estimated if the attenuation of the medium is known by finding the value of a_{eff} that minimizes the average squared difference (*ASD*) given by [*Insana et al.*, 1990]

$$ASD = \underset{\omega}{\text{mean}}\left[\left(X\left(\omega, a_{eff}\right) - \overline{X}\left(a_{eff}\right)\right)^2\right], \tag{2.75}$$

where

$$\begin{aligned} X\left(\omega, a_{eff}\right) &= \ln\left(\frac{\mathrm{E}\left[\left|V_{refl}(\omega)\right|^2\right]}{\left|V_{plane}(\omega)\right|^2 k_o^4}\right) + \ln\left(A_{comp}(\omega)\right) - \ln\left(F_\gamma\left(f, a_{eff}\right)\right) \\ \overline{X}\left(a_{eff}\right) &= \underset{\omega}{\text{mean}}\left[X\left(\omega, a_{eff}\right)\right]. \end{aligned} \tag{2.76}$$

Any errors in the attenuation using the traditional estimation scheme will produce errors in the resulting scatterer size estimate. As a result, the traditional estimation scheme has only been successful when the attenuation of the medium is negligible, such as in *Lizzi et al.'s* [1983] work diagnosing optical tumors.

2.3 Chapter Summary

In this chapter, the effects of focusing on estimating the size of scatterers in random media were considered. The analysis assumed that the velocity potential field near the focus can be modeled as a three-dimensional Gaussian beam, the scatterers are a sufficient distance from the source, and the field is approximately constant across the scatterer. The derivations demonstrated that correcting for focusing along the beam axis when obtaining estimates of scatterer size requires a generalized attenuation-compensation function that includes attenuation, windowing, and diffraction. Furthermore, the results provided insight into the applicability and robustness of previous attenuation-compensation functions in light of diffraction along the beam axis. The theoretical work was also extended to diagnostically relevant fields where the transmit and receive foci are not necessarily at the same depths. After deriving the theoretical equations, the traditional algorithm for estimating scatterer size when the attenuation along the propagation path and in the scattering region is known was discussed.